Towards a sustainable approach for sound absorption assessment of building materials: Validation of small-scale reverberation room measurement

(Article begins on next page)

17 April 2024

1 **Towards a sustainable approach for sound absorption assessment of building materials:**
2 **validation of small-scale reverberation room measurements** [a]
3

4 Authors: Louena Shtrepi[1], Andrea Prato[2]

5 [1]Politecnico di Torino, Torino, Italy

6 [2]INRiM - Istituto Nazionale della Ricerca Metrologica, Torino, Italy

7
8 e-mail addresses: louena.shtrepi@polito.it, a.prato@inrim.it

9
10 Corresponding author: Louena Shtrepi

11 E-mail address: louena.shtrepi@polito.it

12 Postal address: Department of Energy (DENERG), Corso Duca degli Abruzzi 24, 10129, Torino,

13 Italy

Abstract

The research and development phase of sound absorptive building materials by designers, engineers, acoustic consultants and architects need tools for fast, inexpensive preliminary comparison tests on products or acoustic systems. The existing methods exhibit some drawbacks: the impedance tube (IT) is not suitable for 3D systems, while the full-scale reverberation room (FSRR) requires test samples of large dimensions. To overcome these limitations, this work aims to explore the capabilities of small-scale reverberation rooms (SSRR) of about 3 m^3 located at Politecnico di Torino in evaluating the random-incidence sound absorption coefficient. In order to define the range of application and reliability of the method, the considered factors are the sample area and its orientation on the room floor. Four different materials have been tested by applying IT, FSRR and SSRR. The absorption coefficients data obtained with SSRR are compatible with the FSRR benchmarking in the 400-5000 Hz frequency range for three porous materials, and in the range 1000-5000 Hz for the thin rigid material. Therefore, the SSRR can be considered as a reliable alternative for the sound absorption characterization in these ranges for this kind of materials, leading to several benefits. Among them, samples with reduced size can be evaluated with a cheaper equipment in a short time, increasing the overall economical sustainability of the measurement process; in turn, this can encourage designers and architects to perform acoustical measurements since the very early research and development phase, leading to an overall reduction of design costs and improved product quality.

1. Introduction

The design process of sound absorptive materials is complemented by a preliminary exploratory phase that requires an immediate feedback on the acoustic performance, i.e. the absorption coefficient. Therefore, adequate tools are needed to accelerate the research and development process, minimize costs, and reduce waste due to dismantled samples after their characterization. The absorption coefficient measurement procedure has been the focus of continuous research that have led to two main standardized methods, i.e. the impedance tube (IT) method defined in ISO 10534 [1] and the full-scale reverberation room (FSRR) method described in ISO 354 [2] and ASTM Standard C423 [3]. However, these methods present several disadvantages: IT does not allow to test 3D systems, while FSRR requires large samples. This paper aims to explore the capabilities of small-scale reverberation rooms (SSRR) in providing accurate estimations of the absorption coefficients with respect to the FSRR benchmarking and in overcoming the above-mentioned drawbacks of existing methods.

The main advantages of a SSRR are the possibility to test samples that are much smaller than 10-12 m^2 and the 6.69 m^2 recommended by the FSRR measurements (V>200 m^3) according to ISO 354 [2] and ASTM Standard C423 [3], respectively, and to allow more acousticians, manufacturers and practitioners to build their test facility due to the more feasible construction compared to a FSRR. This, in turn, enables a dramatic reduction of economical and time efforts necessary to perform a FSRR measurement. Moreover, the SSRR can be used to improve the quality of acoustic simulations: novel materials at configurations not available in existing databases can be characterized much more easily [4].

Due to their cost effectiveness, SSRRs have been the focus of research in the automotive sector [5], which usually requires absorption data at medium-high frequencies due to the small size of the involved samples. The research has led to a SAE (Society of Automotive Engineers) standard [6] on the use of small rooms for absorption coefficients measurements. The common size of these rooms

64 is in the range of 3-10 m^3, and a sample area of 0.4-1.5 m^2 is usually deployed [7]: this leads to

65 nearly 90% reduction of the wasted material for laboratory measurements compared to the FSRR

66 (12 m^2). The sample arrangement in the SSRR requires a shorter set-up time: a single panel is

67 usually sufficient, while in FSRR several panels need to be assembled to reach a 12 m^2 sample. In

68 turn the transportation costs and the related environmental pollution benefit from the reduction in

69 material volume. Moreover, the same samples could be reused to measure other important

70 properties for building materials, e.g. the thermal conductivity [8], since the required sample

71 dimensions are comparable to those used in small-scaled rooms.

72 Further SSRRs are reported in Rey et al. [9] with a volume of 1.12 m^3 and test sample area of 0.3

73 m^2, and Pacheco et al. [10] with a volume of 0.96 m^3 and test sample area of 0.3 m^2. These scaled

74 rooms have been useful also for testing more complicated structures, e.g. 3D rigid polyester

75 systems, which is difficult to test in an impedance tube [11]. The continuous research on SSRRs has

76 led to the Alpha Cabin, built by the Swiss company Rieter, with a volume of 6.5 m^3. The design and

77 size of the Alpha Cabin is 1:3 scale of the large reverberation room located in the Swiss Federal

78 Laboratory of Material Testing and Research Institute (EMPA). It is largely used in the automotive

79 industry allowing to measure 1.2 m^2 of flat samples or 3D moulded finished parts providing

80 accurate measurements in the frequency range of 400-5000 Hz [11].

81 A few studies have also compared small-scale reverberation room measurements with those

82 performed in a full-scale reverberation room [9, 11-13]. A good match of the results has been

83 shown in the range of frequencies above 400 Hz, where the SSRR is expected to fulfil the perfect

84 diffusion conditions, i.e. where the degree of diffusion is close to 1. However, these studies also

85 highlight larger discrepancies at low frequencies due to the reduced size of the room. This is a

86 critical aspect since the resulting smaller sample area with equal height produces a larger edge

87 effect [14, 15]. The impact of these effects is particularly high at low frequencies if highly

88 absorbing materials with high thicknesses are tested.

89 Therefore, two main concerns appear when dealing with small reverberation rooms. The first is

90 related to the lack of a degree of diffusivity of the sound field required to make the measurement

91 conditions largely independent of the room properties [16]. To mitigate this issue, usually different

92 types of diffusers are introduced [2, 17,18]; nevertheless, the efficiency of the diffusers is shown to

93 be reduced when the frequency decreases [19]. In addition, according to Scrosati et al. [20], the

94 diffusers change the mean free path in the reverberation room, thus ISO 354 formula for the

95 calculation of the equivalent absorption area is no longer valid since it does not take into account

96 the actual mean free path and consequently the changed volume of the room. However, low

97 diffusivity of reverberation rooms is still one of the main concerns of the ISO 354 measurements

98 related to the low reproducibility values among laboratories. This is much evident at low

99 frequencies [21], but appear even above the Schroeder frequency, where the sound field should

100 reach a higher degree of diffusivity [22, 23]. One of the causes is due to the fact that the sound field

101 is diffuse in the empty room, while in the room with a highly absorbing sample the sound field

102 cannot be considered perfectly diffuse [20]. For this reason, the diffuse field conditions differences

103 among laboratories has been questioned lately aiming at new requirements to be defined in terms of

104 diffusivity for qualified laboratories [24]. Several studies have shown that large discrepancies might

105 occur among different full-scale laboratories even though they fulfil the ISO qualification

106 requirements [25]. As for FSRR, the low frequencies range in SSRR is the most critical one, where

107 the early decay is dependent on strong, distinct reflections and need to be treated with specific

108 methods [26, 27].

109 The second drawback of SSRR measurements is related to the diffraction due to the finite size of

110 the tested material, especially at the low frequencies, which is known as the edge effect [14, 28, 29],

111 and restricts the reliability frequency range at medium-high frequencies. Further investigation is

112 needed to clarify the trade-off between reduced sample size and the appropriate room and sample

113 conditions to obtain reliable results for building materials.

To shed light in this direction, this study examines a broad measurement campaign in a small-scale reverberation room in the laboratories of the Department of Energy (DENERG) of Politecnico di Torino, with the aim to evaluate the reliability of the sound absorption coefficient measurements. Four different materials at three different sizes and orientations on the room floor have been tested. The work assesses the compatibility of the SSRR measurements towards measurements made on the same materials in a full-scale reverberation room (ISO 354) [2] at INRiM (Istituto Nazionale di Ricerca Metrologica). Moreover, the same materials have been additionally characterized with the impedance tube method (ISO 10534-2) [1] in order to present an easier and direct comparison towards another standardized method. Finally, the single sound absorption indices α_w (weighted sound absorption coefficient), NRC (Noise Reduction Coefficient), and SAA (Sound Absorption Average), which are used to assess the quality of the absorption and to select products by designers and architects, are derived from the three measurement methods.

2. Methods

The research has been organized through the following steps:

1) Selection of materials and preparation of samples for the measurements in IT, FSRR and SSRR;

2) Measurement of sound absorption in the IT according to ISO 10534-2 [1] and FSRR according to ISO 354 [2];

3) Measurement of sound absorption in the SSRR and test the range of application of ISO 354 [2] method by varying the area of the sample and its orientation on the room floor;

4) Evaluation of the compatibility of the measured SSRR data with the results from IT and FSRR;

5) Computation of the indices α_w, SAA and NRC for the IT, FSRR and SSRR data and compatibility assessment.

2.1 Tested Materials

140   Four materials (here labelled A, B, C, D) available at INRiM have been tested (Figure 1). Materials

141   A and B are made of glass wool panels with a density of 80 kg/m^3 and a 6 mm finished layer made

142   of glass spheres and a marble powder with overall thickness of 40 mm and 50 mm, respectively.

143   Material C is a 21 mm thick panel with a layer of 13 mm of plasterboard and 8 mm finished layer

144   made of a marble powder. Material D is composed of two superimposed layers of polyester fibre

145   with a density of 80 kg/m^3 and a thickness of 30 mm each. Also, this material has a cellular glass

146   finish of 7.5 mm over the upper layer, and a mixture of rubber and concrete layer of 7.5 mm at the

147   bottom. Since all these materials are obtained by layers of different characteristics, they can be

148   considered as non-isotropic. The four materials have been chosen based on commercially available

149   materials in order to have four different thicknesses: two similar materials A and B with the same

150   layers characteristics but with slightly different thickness, material C considered as a thin rigid

151   material and material D was chosen in order to test the SSRR also for significant thicknesses.

A	B	C	D
Glass wool panels with a finish of 6 mm of glass spheres and a marble powder	Glass wool panels with a finish of 6 mm of glass spheres and a marble powder	Panel with a layer of plasterboard and one of 8 mm of marble powder	Double layered Polyester fiber panel; cellular glass finish of 7.5mm over the upper layer, and a mixture of rubber and concrete layer of 7.5mm at the bottom
Thickness: 40mm	Thickness: 50 mm	Thickness: 21 mm	Thickness: 75 mm
Mass density per unit area: 7.30 kg/m²	Mass density per unit area: 7.70 kg/m²	Mass density per unit area: 14.15 kg/m²	Mass density per unit area: 7.10 kg/m²

152

Fig. 1. Sample A and B: Glass wool panels with a finish of glass spheres and a marble powder (40 mm and 50 mm). Sample C: one layer of plasterboard and one of marble powder (21 mm). Sample D: Double layered polyester fibre panel with a cellular glass finish (75 mm).

2.2 Impedance tube measurements

Measurements have been performed in the impedance tube in accordance with ISO 10534-2 [1] (two-microphone technique) in order to measure the normal-incidence absorption coefficient (α_0) for the four materials. The advantages of this method rely on the possibility to obtain measurements using small samples of less than 0.1 m^2 that are easily obtained and introduced into the impedance tube. These measurements took place in the INRiM laboratory. Two different tubes of 30 mm and 50 mm diameter each (Figure 2), both equipped with two ¼'' microphones (Brüel & Kjær 4136), have been used in order to assure a higher accuracy in the whole frequency range of interest, i.e. 100-5000 Hz. The 30 mm tube (length of 45 cm and microphone spacing of 16 mm) allows to measure with a high accuracy in the frequency range of 400-6300 Hz and the 50 mm tube (length of 52 cm and microphone spacing of 26 mm) in the frequency range of 100-3150 Hz. The ISO 10534-2:2001 standard does not define the exact frequency range for a given tube diameter and microphone separation, but recommends the bounds for the lower and upper frequencies; therefore, the frequency range was chosen to satisfy the standard requirements for the level of nonlinearities, frequency resolution, measurement instabilities and signal-to-noise ratio [30].

Both the two tubes are equipped with a white noise source which generates a flat spectrum in the 100-5000 Hz frequency range. The possible gaps among the sample perimeter and the tubes inner surfaces have been sealed by covering the sample border with vaseline without creating local compression on the samples. In this way, the size of the voids between the tested material and the sample holder was reduced so that the circumferential effect discussed in [31] could be considered negligible. The effect of the irregularities in the samples, and in particular at the edges, was taken

178   into consideration by repeating the tests with three different samples. Temperature and atmospheric

179   pressure were measured with proper calibrated transducers. For each material type, measurements

180   were performed on three samples (nominally equal), obtained from the same larger sample, in order

181   to evaluate uncertainty contribution due to reproducibility.

182   The normal-incidence absorption coefficients (α_0) data from the two tubes measurements have been

183   combined in order to fulfil their covered frequency range, thus considering the values from the 50

184   mm tube in the range 100-315 Hz; the mean values from the two tubes in the range 400-3150 Hz

185   and the values from the 30 mm tube in the range 4000-5000 Hz. These data are shown in

186   Appendices A, B, C and D as IT_n.

187   These values have been corrected for diffuse incidence based on the approach proposed in Spagnolo

188   and Benedetto [32], which uses a physical model to determine the random-incidence absorption

189   coefficient (α) by integrating a vector of evenly spaced 90 angles between 0° and 90°, i.e. the whole

190   hemi-solid angle, allowing to estimate the sound energy density absorption at each angle of

191   incidence, randomly, as in near-diffuse field, according to Eq. (1). There are several methods that

192   can be used to perform this correction taking into account the finite sample size [33] and a different

193   angular integration limit [34].

$$\alpha = \int_0^{\pi/2} \alpha_\theta \, cos\theta \, d\theta \tag{1}$$

194

195   where θ is the angle of incidence of the pressure waves on the sample and α_θ is the sound

196   absorption coefficient at angle θ given by Eq. (2);

$$\alpha_\theta = 1 - \left| \frac{Zcos\theta - \rho_0 c}{Zcos\theta + \rho_0 c} \right|^2 \tag{2}$$

197

198   where Z, assuming locally reacting surface, is the acoustic impedance of the absorbing material

199   given by:
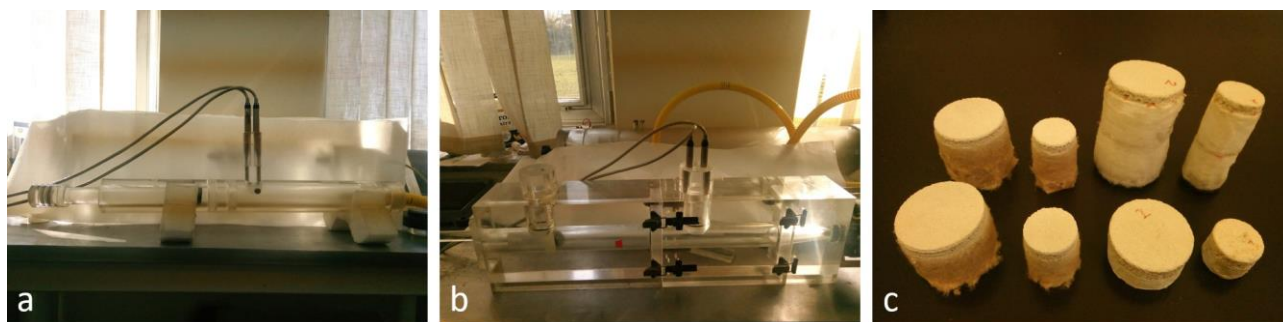
$$Z = \rho_0 c \frac{1 + (1 - \alpha_0)^{1/2}}{1 - (1 - \alpha_0)^{1/2}} \tag{3}$$

200

201   where ρ_0 is the density of air, c is the speed of sound, and α_0 is the normal-incidence absorption

202   coefficient evaluated in the impedance tube.

203

204

205   **Fig. 2.** Measurements set-up in the impedance tube with a diameter of a) 30 mm and b) 50 mm, and

206   c) circular samples of the four materials with a diameter of 30 and 50 mm.

207

208   *2.3 Full-scale reverberation room measurements*

209   All the materials have been tested in the full-scale reverberation room at INRiM, which is a

210   qualified room for measurements in accordance with ISO 354 [2]. The method allows to estimate

211   the random-incidence absorption coefficient (α_S) in the 100-5000 Hz frequency range. The room

212   has a floor surface of 59.4 m^2 and a height of 4.95 m, which lead to a volume of 294 m^3. Room plan

213   is irregular with non-parallel side walls. The indoor surfaces are characterized by strongly reflective

214   walls and a marble floor characterized by an equivalent sound absorption area lower than 5 m^2 in

215   the 100-5000 Hz frequency range. The mean reverberation time of the empty room between 100 Hz

216   and 5000 Hz is of 10.3 s, thus the Schroeder frequency f_s is 374 Hz. Five diffusers are hung over the

217   ceiling in order to assure diffusivity. The tested samples have an area of 12 m^2 and have been

218   located on the floor of the room within a wooden frame, which is recommended to be used to seal

219   the edges of the tested material. In this experiment the frame has been used for all the samples

except for the case of sample C, which has a negligible thickness. The porous layer for this material is of 8 mm, which was taken into account in the estimation of the overall area of the sample by increasing it of 0.11 m^2.

The set-up and the samples of each material have been arranged in accordance with the recommendations of the ISO 354 standard (Figure 3):

- microphones should be positioned at a minimum distance of 1.5 m from each other, 1 m from the room surfaces and 2 m from the sources;
- the two sources must be at least 3 m apart from each other. A spatial averaging is performed considering all the 12 sources and microphones combination;
- the interval of frequencies of interest is reported as third-octave bands in the range 100-5000 Hz;
- controlled conditions of temperature (> 15 °C) and humidity (between 30-90 %);
- the sample must be rectangular with a ratio between width and length within the range 0.7-1. In this specific case, the test specimens were composed of 25 single small panels with size 60×80 cm^2 combined in order to cover an area of 4×3 m^2;
- the sides of the sample must be distant from the walls of the room by at least 1 m.

Fig. 3. Measurements in the full-scale reverberation room a) without and b) with the sample.

240   The procedure consists in using the interrupted noise method [2] on six different microphone

241   positions in two conditions, i.e. with and without the sample on the floor of the room. The

242   measurement chain is composed of a 1/2" microphone (Brüel & Kjær 4943), sequentially located at

243   different positions, and two dodecahedral sources (Brüel & Kjær 4292 and Brüel & Kjær 4296).

244   The applied recording system is the SINUS, Apollo system with software Samurai 2.6; while the

245   sound equalizer is Yamaha (DEQ 5) and the power amplifier is Amcron Crown (MICRO-TECH

246   1200). In these measurements two sound sources are used for the simultaneous excitation, therefore

247   the number of spatially independent measured decay curves may be reduced to six [2]. For each of

248   the six positions, measurements are repeated four times, and the reverberation time relative to a 20

249   dB decay, i.e. T_{20}, is evaluated and used to estimate the T_{60}, i.e. the reverberation time occurring for

250   a 60 dB decay. The data are spatially averaged with the ensemble averaging method in order to

251   obtain T_1 and T_2 without and with the sample on the room floor, respectively. The difference

252   between the two measures is used to calculate the variation of the equivalent sound absorption area

253   A_T based on Sabine's theory:

$$A_\text{T} = 55.3V \left(\frac{1}{c_2 T_2} - \frac{1}{c_1 T_1} \right) - 4V(m_2 - m_1) \tag{4}$$

254

255   where T_1 and T_2 are the reverberation times of the empty reverberation room and after the test

256   specimen has been introduced, respectively; V is the volume of the empty reverberation room; c_1

257   and c_2 is the propagation speed of sound in air in the room without the sample: $c_1 = 331 + 0{,}6\ t_1$, t_1

258   is the air temperature; m_1 and m_2 is the power attenuation coefficient of the climatic conditions in

259   the reverberation room without and with the sample (calculated according to ISO 9613-1 [35]);

260
261   The random-incidence absorption coefficient is defined as:

$$\alpha_\text{S} = \frac{A_T}{S} \tag{5}$$

262

263 Where S is the area covered by the test sample.

264

265 *2.4 Small-scale reverberation room measurements (SSRR)*

266 The small-scale reverberation room (Figure 4, a and Figure 5) is a laboratory at DENERG

267 (Department of Energy, Politecnico di Torino, Italy). It is a 1:5 scale reproduction of the

268 reverberation room described above. The room has been primarily built for random-incidence

269 scattering coefficient measurements according to ISO 17497-1 [36, 37]. It is an oblique angled

270 room with pairs of nonparallel walls. The floor area is about 2.38 m^2 and the height in the range 1-

271 1.2 m, which lead to a maximum volume of 2.86 m^3 and a total area of 12.12 m^2. The structure is

272 raised from the ground on a wooden structure and damping layers have been used along the joints

273 and openings. One of the sides consists of two movable parts that allow to have a large opening to

274 ease the positioning of the sample. The construction material is self-supporting lightweight

275 partitions of MDF (Medium Density Fibreboard) with a thickness of 3.8 cm, which has been further

276 covered by a layer of adhesive film in order to maximize its reflective properties. The equivalent

277 sound absorption area of the empty room (A_1) and ISO [2] and ASTM [3] limits are shown in

278 Figure 4, c. The ISO limit values have been multiplied by the factor $(V/200)^{2/3}$, while the ASTM

279 limit value is given in terms of mean absorption coefficient ($\alpha_m \leq 0.05$ in the 250-2500 Hz interval,

280 and $\alpha_m \leq 0.10$ below 250 Hz and above 2500 Hz) and has been converted into equivalent sound

281 absorption area for comparison purposes. Given that the ISO limit is not specifically indicated for

282 rooms below a volume of 150 m^3, A_1 can be considered acceptable even though slightly above the

283 limit in the range 800-1600 Hz. However, the average absorption coefficient of the indoor surfaces

284 is lower than $\alpha_m = 0.05$ in the frequency range of interest (100-5000 Hz). The mean reverberation

285 time of the empty room between 100 Hz and 5000 Hz of 0.95 s, thus the Schroeder frequency f_s is

286 1152 Hz.

287 In order to assure a high diffusivity of the sound field [38], 8 diffusers (13.5% of the total room

288 area) have been hung over the ceiling, which is considered as a more economical solution compared

289   to boundary diffusers leading to an almost equivalent effect on the diffusion of the sound field [18].

290   A systematic study of the sound field diffusivity evaluation of the room has been performed in [39].

291   The diffusivity check has been performed in accordance with ISO 354 based on the measurements

292   of the mean absorption coefficient (500-5000 Hz) of a highly sound absorptive panel made of 5 cm

293   thick polyester fibre (Figure 4, d). The final number of diffusers was set to 8, which was a

294   compromise between the rule set by the standard i.e. the mean sound absorption coefficient

295   approaches a constant value (6D to 8D), and limited effect on the volume reduction of the room due

296   to the total coverage of the ceiling, i.e the condition with 10 diffusers (10D).
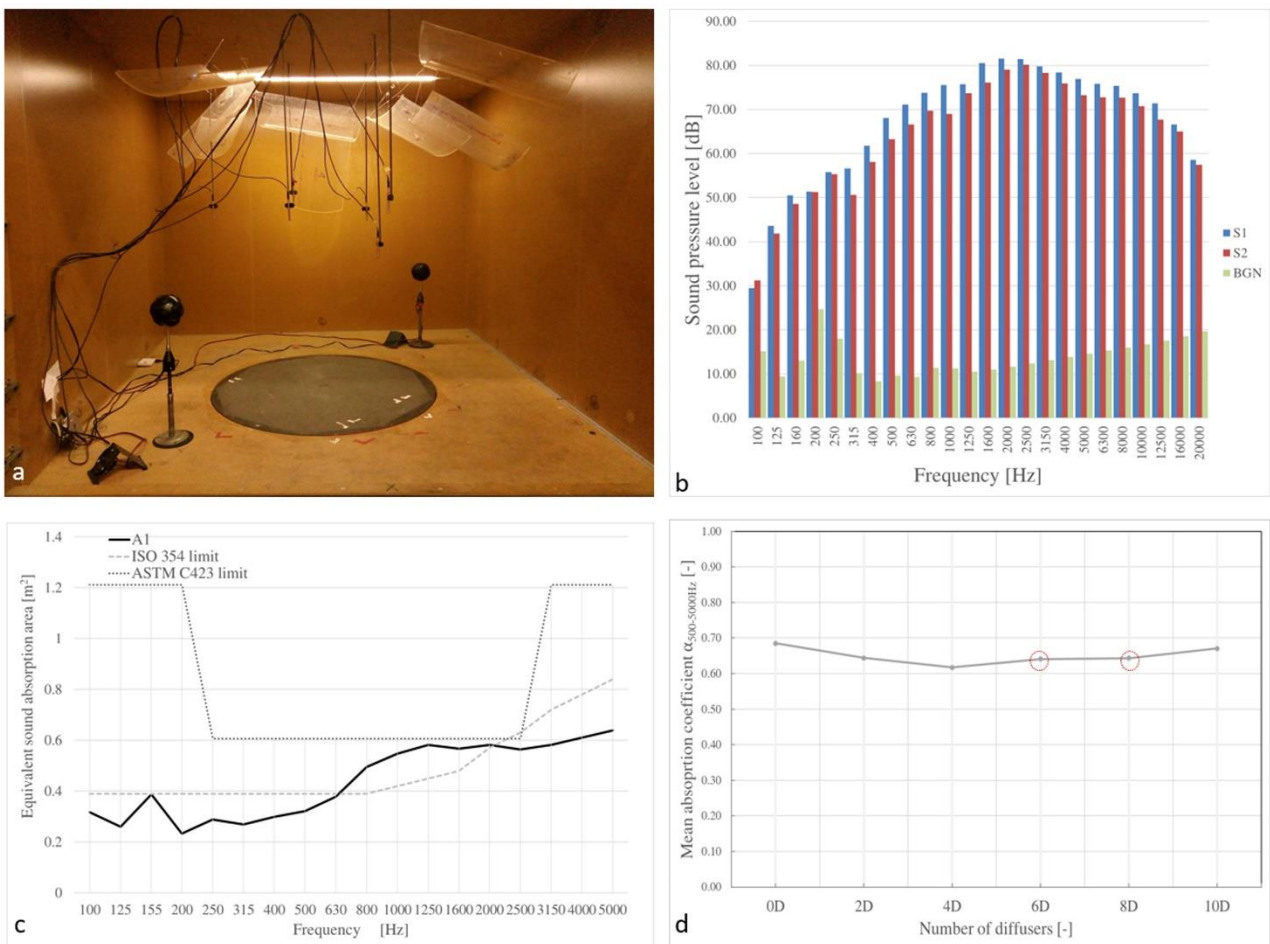
297

298   **Fig. 4.** a) Empty small-scale reverberation room; b) spectral characteristics of the two sound sources

299   (S1 and S2) and background noise; c) comparison of the equivalent sound absorption area of the

300   empty room (A_1), ISO and ASTM limits; d) mean absorption coefficient of a polyester panel of 5

301   cm measured in the room with no diffusers (0D) and 2-10 diffusers (2D-10D).

13

302

The procedure consists in using the integrated impulse response method [2] for simultaneous measurements on six different microphone positions in two conditions, i.e. with and without the sample on the floor of the room as in section 2.3. The measurement chain is composed of six 1/4" BSWA Tech MPA451 microphones and ICP104 (BSWA Technology Co., Ltd., Beijing, China); two ITA High-Frequency Dodecahedron Loudspeakers with their specific ITA power amplifiers (ITA-RWTH, Aachen, Germany) and a sound card Roland Octa-Capture UA-1010 (Roland Corporation, Japan) in order to perform 12 measurements (the minimum number required by ISO 354 [2]). The software used for the measurements, i.e. sound generation, recording and signal processing, is MATLAB combined with the functions of the ITA-Toolbox (an opensource toolbox from RWTH-Aachen, Germany) [40]. The sound source should fulfil the ISO 354 spectral characteristics, that is, the sound pressure levels in the room shall be less than 6 dB in adjacent one-third-octave bands and the level of the excitation signal before the decay shall be sufficiently high so that the lower decibel level of the evaluation range is at least 10 dB above the background noise level, i.e. 35 dB below the initial sound pressure level. The first criterion is fulfilled for the entire frequency range, while the second is fulfilled only above the 250 Hz (Figure 4, b).

For each of the 12 measurements the reverberation time is evaluated. The data are spatially averaged in order to obtain T_1 and T_2 without and with the sample on the room floor, respectively. Equations 4 and 5 are then applied to estimate the random-incidence absorption coefficient.

The set-up and the samples of each material have been arranged in agreement with the recommendations of the ISO 354 standard (Figure 5):

- "microphones should be positioned at a minimum distance of 1.5 m from each other, 1 m from the room surfaces and 2 m from the sources". This leads to 0.3 m; 0.2 m and 0.4 m in 1:5 scale;

- "the two sources must be at least 3 m apart". This leads to 0.6 m in 1:5 scale. A spatial averaging is performed considering all the 12 sources and microphones combination;

- the frequencies of interest are reported as third-octave bands in the range 100-5000 Hz. Given the background noise criterion, this is valid for 250-5000 Hz;

- controlled conditions of temperature (> 15 °C) and humidity (between 30-90 %). A sensor has been installed inside the room;

- "the sides of the sample must be distant from the walls of the room by at least 1 m". This leads to 0.2 m in 1:5 scale;

2.4.1 Sample configuration

One of the aims of this study is to define the sample configuration that could lead to accurate results of the absorption coefficient measurements in the small-scale reverberation room. Given the small size of the SSRR, the sound field is expected to be strongly dependent on the configuration of the measured material. Therefore, it is crucial to define the application range of this type of measurements.

The following variables have been considered, tested and the results have been compared with the IT and FSRR measurements:

- three different sample seizes for each material (60×40 cm^2; 60×60 cm^2; and 60×80 cm^2). It should be noted that the ISO 354 recommends a ratio between width and length in the range 0.7-1;

- three different orientations on the floor (Fig.5) for the 60×40 cm^2 and 60×80 cm^2 sample sizes and two different orientations for sample 60×60 cm^2. Orientation 1 assumed the long edge of the sample parallel to the side wall, orientation 2 assumed the axis of symmetry of the sample aligned over the diagonal of the room floor giving an oblique orientation, and

350   orientation 3 assumed the long edge of the sample parallel to the rear wall. It should be

351   noted that the ISO 354 standard recommends an oblique orientation (orientation 2).

352   Three repetitions have been performed for each configuration.
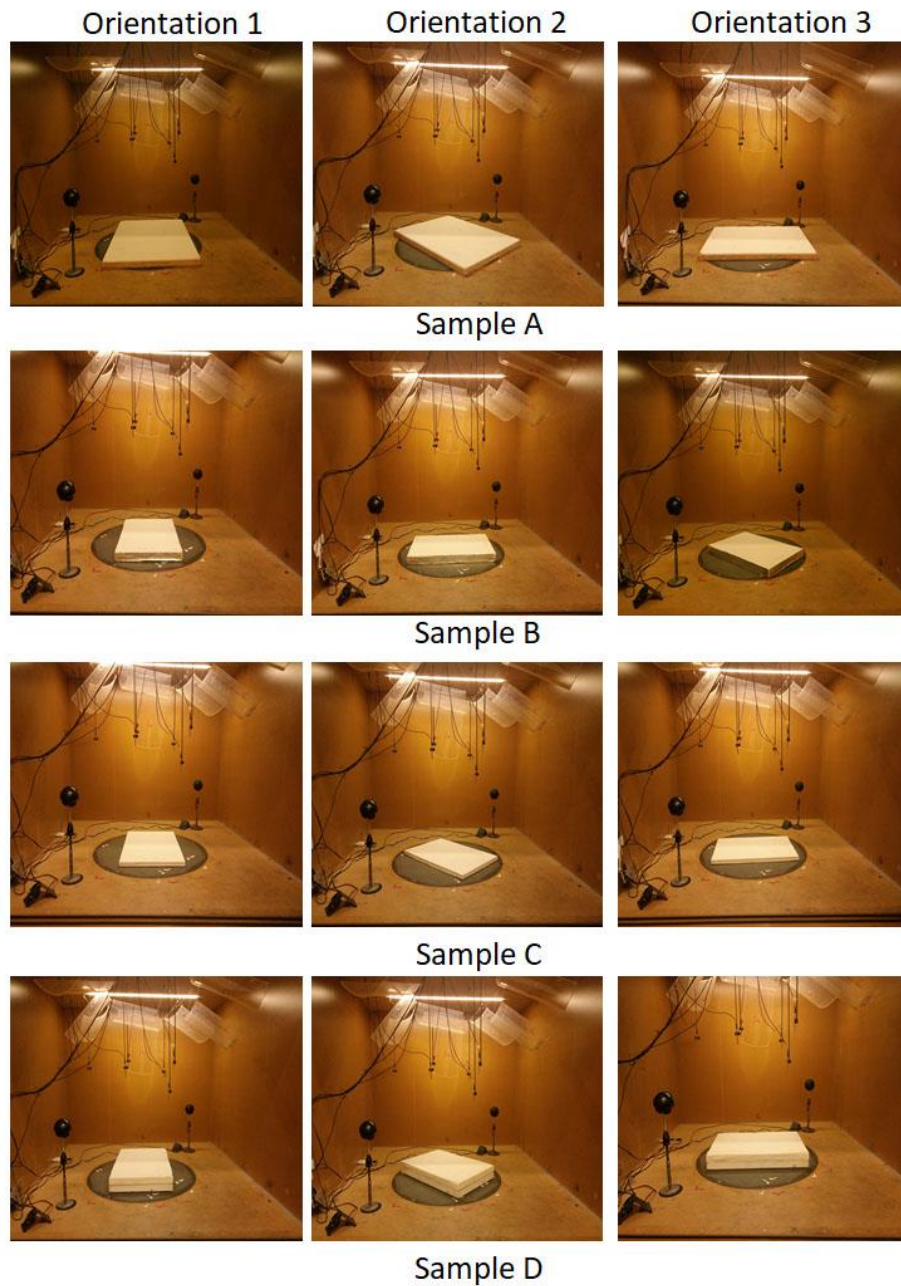
Fig. 5. Measurements in the small-scale reverberation room of one of the samples with three different orientations; Sample A (60×80 cm^2), Sample B (60×40 cm^2), Sample C (60×40 cm^2) and Sample D (60×40 cm^2).

3 Analyses

An analysis based on the estimation of the normalized error (E_n) has been performed in order to assess the compatibility of the absorption coefficient data measured in the SSRR with respect to the FSRR ($E_{n,FSRR}$), considered as reference value for random incidence sound absorption, and IT extended for random-incidence absorption coefficients ($E_{n,IT}$). Moreover, also the normalized error of IT results has been assessed with respect to the FSRR values. E_n is defined as the ratio of the difference between the reference value (α_x) and the reported value (α_y) compared to the root sum square of associated expanded uncertainties (U_x and U_y) at a confidence level of 95% ($k=2$). According to ISO/IEC 17043:2010 [41], it is evaluated as follows:

$$E_n = \frac{|\alpha_x - \alpha_y|}{\sqrt{U_x^2 + U_{xy}^2}} \tag{6}$$

The data can be considered compatible when $E_n < 1$. This is an indicator of accuracy/inaccuracy as compared to an assigned reference value (FSRR or IT) with respect to the associated uncertainties. The uncertainty of the impedance tube measurements has been assessed according to GUM-JCGM 100:2008 [42]), taking into account, as type B uncertainty contribution, the difference between the maximum and minimum values coming from the measurement on three nominally equal samples with a uniform rectangular distribution. The specific guidelines given by Wittstock (2018) (see Eq. (2) and Table II – smooth case) [43], which are currently the most reliable reference for the uncertainty evaluation in reverberation rooms based on a database of Interlaboratory Tests, have been applied for the SSRR and FSRR measurement uncertainties. Nevertheless, as shown by the author itself [43], larger uncertainties might occur, especially for highly absorptive materials with ISO 354 method, thus entailing a possible underestimation of the E_n values. Such aspect should be taken into account in the conclusions. The measured frequency dependent absorption coefficients of the four materials and the estimated measurement uncertainties are shown for further details in Appendices A, B, C and D.

381   The normalized error data have been further analysed with a focus on the effects of the independent

382   factors, i.e. the sample size and orientation. The SPSS Statistics software [44] has been used to

383   perform the ANOVA (ANalysis Of VAriance). The data have been first analysed with a normality

384   test (Kolmogorov-Smirnov test): $E_{n,IT}$ showed a skewness of 0.793 (std.error = 0.105) and kurtosis

385   of 0.004 (std.error = 0.210); $E_{n,FSRR}$ showed a skewness of 0.793 (std.error = 0.105) and kurtosis of

386   0.004 (std.error = 0.210), thus falling within the acceptable range of ±2 [44].

387   Moreover, the single indices for sound absorption (α_w, NRC and SAA) are derived from the IT,

388   FSRR and SSRR measurements and compared in terms of compatibility.

389

390   Table 1: ANOVA results for $E_{n,IT}$ and $E_{n,FSRR}$ data set.

	$E_{n,IT}$				$E_{n,FSRR}$			
	Size		Orientation		Size		Orientation	
Material	F	p	F	p	F	p	F	p
A	(2, 135) 21.580	0.000	(2, 135) 0.095	0.910	(2, 135) 15.248	0.000	(2, 135) 0.110	0.896
B	(2, 135) 13.910	0.000	(2, 135) 0.093	0.980	(2, 135) 5.496	0.005	(2, 135) 0.090	0.914
C	(2, 135) 0.827	0.440	(2, 135) 0.468	0.628	(2, 135) 0.501	0.607	(2, 135) 0.235	0.791
D	(2, 135) 5.481	0.005	(2, 135) 0.308	0.736	(2, 135) 20.018	0.000	(2, 135) 0.255	0.776

391

4 Results and discussion

4.1 Effects of the independent factors

The ANOVA performed on the overall E_n set of data showed that the four materials are significantly different from each other at a confidence level of 95% for $E_{n,IT}$ with respect to IT (F (3, 540) = 14.143 and p < 0.001) and at a confidence level of 90% for $E_{n,FSRR}$ with respect to FSRR (F (3, 540) = 2.277 and p = 0.079). Therefore, sample size and orientation variables have been analysed for each material separately (Table 1).

The effect of the sample size is statistically significant for all the samples typologies ($p < 0.05$), except for sample C. This result might be due to the limited edge effect for thinner samples, as sample C is 21 mm thick. Appendices A, B, C and D show the absorption coefficient values for each material. For panels with higher thickness (i.e. A, B, D) and when the panel reaches the smallest dimensions 60×40 cm^2, there are evident irregular high peaks at mid and high frequencies for panels A and B, and also at low and mid frequencies for panel D. It can be noticed that the sound absorption increases at 160-400 Hz and above 800 Hz with decreasing samples size (Appendices A, B, and D). This behaviour might be due to a combination of edge effects and to diffusivity effects, caused by the influence of the material on the modal behaviour of the room with and without the sample inside, whereas for low absorbing materials (Appendix C) it can be considered equivalent in terms of spatial distribution and amplification of standing waves. Schiavi and Prato [45] showed these discrepancies by comparing full scale reverberation room, impedance tube, and airflow resistivity methods. The same result has been highlighted also in full-scale rooms by Jain et al. [46], for samples size smaller than 1 m^2, which is due to diffraction occurring at the sample edges. Anyway, in general terms, depending on the sample thickness, the small room gives higher sound absorption values as compared to large reverberation rooms [15]. Samples A, B and D showed this trend above 800 Hz, while sample C above 2000 Hz.

19

416   The correct scaling of the sample size with respect to the room volume has been investigated also in

417   Veen et al. [28]. This study shows that a sample of 1.12 m^2 could be considered in order to have

418   reliable results in a small reverberation room with a volume of about 6.4 m^3. The ratio between the

419   room volume and the sample area is comparable to the one obtained with the room volume of

420   2.86 m^3 and the sample size 60×80 cm^2 (0.48 m^2) used in the present study (i.e. ratio ≈ 6).

421   The effect of the sample orientation has been analysed for all the materials and all the sample sizes.

422   Table 1 shows that the differences due to sample orientations are not statistically significant for all

423   the materials considered ($p > 0.05$). It is therefore possible to choose an oblique panel orientation

424   (Orientation 2), as suggested in the standard for full-scale measurements. Previous research [16] has

425   shown that different orientations may cause discrepancies at lower frequencies (below 400 Hz) and

426   that the smoothest curve is obtained for the oblique orientation, which is the most asymmetric one.

427   This study also highlighted that the other two orientations cause strong peaks in the absorption

428   coefficient, which were unrealistic for the tested porous materials. The authors argued that this

429   behaviour might be due to the parallel orientation of two edges of the material against two side

430   walls of the reverberation room. However, this effect is not fully observed in the study presented in

431   this paper. Some differences between the three orientations are observed at specific frequencies for

432   the smallest sample size, i.e. 60×40 cm^2 (Appendixes A, B, C, and D). Discrepancies at lower

433   frequencies are reduced when the material has lower thickness, i.e. these differences are more

434   evident in the case of panel D, which has a thickness of 75 mm. This finding is coherent with the

435   results of Cops et al. [16], which showed the same discrepancies between different orientations for

436   samples with thickness higher than 100 mm in full-scale measurements.

437

438   *4.2* Compatibility of SSRR with IT and FSRR data

439   Figure 6 shows the maximum normalized error values estimated in each third octave band

440   frequency range for the SSRR data with respect to FSRR and IT data. SSRR data are reliable from

441   250 Hz upward, due to the background noise criterion previously discussed, however, for the sake

442   of completeness, results are reported from 100 Hz. These plots show the E_n for material A, B, C and

443   D at three sample sizes (60×40 cm^2, 60×60 cm^2, and 60×80 cm^2) and Orientation 2 only, since this

444   factor was not found to be statistically significant. The results show that the normalized error (E_n) is

445   minimized for sample size 60×80 cm^2 for all the materials. $E_{n,FSRR}$ values are lower than 1 in the

446   frequency range 400-5000 Hz, for materials A, B and D. Sample C presents $E_{n,FSRR}$ values lower

447   than 1 at 400 Hz and in the frequency range 1000-5000 Hz. Values slightly higher than 1 result

448   between 500 Hz and 800 Hz. As highlighted in the previous section, this might be due to the limited

449   effects of this low absorbing and thinnest sample on the modal behaviour of the room it-self. This

450   result suggests further future investigation on the room diffusivity. The same conclusions can be

451   obtained for $E_{n,IT}$ for materials A, B and C. For what concern material D, it can be noted that $E_{n,IT} <$

452   1 only at 500-1000 Hz. This could be due to the fact that IT method tends to underestimate the

453   sound absorption at mid-high frequencies as shown in Appendix and in Figure 6. $E_{n,IT}$ values are

454   higher than $E_{n,FSRR}$ values, which leads to a higher compatibility of the SSRR with respect to the

455   FSRR. These differences are maximized for the thickest material D, i.e. $E_{n,IT} > 1$ and $E_{n,FSRR} < 1$ at

456   1250-4000 Hz. The same behaviour can be observed also when evaluating the normalized error of

457   the IT data with respect to the FSRR (Figure 7), i.e. $E_n > 1$ at 1600-3150 Hz.

458

21

Fig. 6. Normalized error (E_n) for SSRR results (material A, B, C and D) with respect to IT ($E_{n,IT}$) and FSRR ($E_{n,FSRR}$) values for the three sample sizes (60×40 cm^2, 60×60 cm^2, and 60×80 cm^2) and orientation 2. The data can be considered compatible when $E_n < 1$.
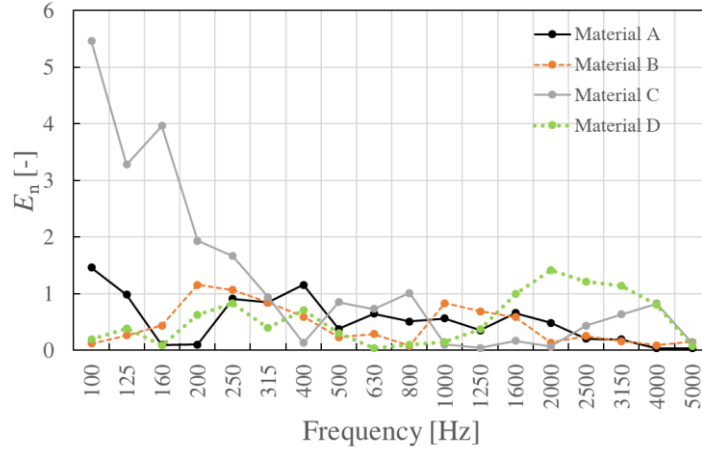
Fig. 7. Normalized error (E_n) for IT results (material A, B, C and D) with respect to the FSRR values. The data can be considered compatible when $E_n < 1$.

The absorption coefficient data of the optimal condition i.e. size 60×80 cm^2 and sample orientation 2, together with the uncertainty values of the results, are shown in Figures 8. The plots show that the SSRR values tend to be higher for frequencies above 800 Hz for samples A, B and D and above 2000 Hz for sample C. One of the causes for this behaviour is that the absorption coefficient approaches to 1 at these frequency ranges and influences the diffusivity of the sound field generated within the small-scale room. This has been observed also in Veen et al. [28], where higher discrepancies around 1000 Hz for samples with thickness above 25 mm were found. Also, Jain et al. [46] showed a good match at mid frequencies from 400-1000 Hz between FSRR and SSRR and an overestimation of sound absorption values above 1000 Hz for the small-scale reverberation room. This is attributed to the use of Sabine's formulas instead of Eyring's as highlighted by Vercammen [21]. Moreover, it should be highlighted that the differences obtained here between the small- and

22

477   full-scale room or impedance tube measurements are comparable with those obtained from

478   absorption coefficient measurements in 13 different laboratories Vercammen [21].
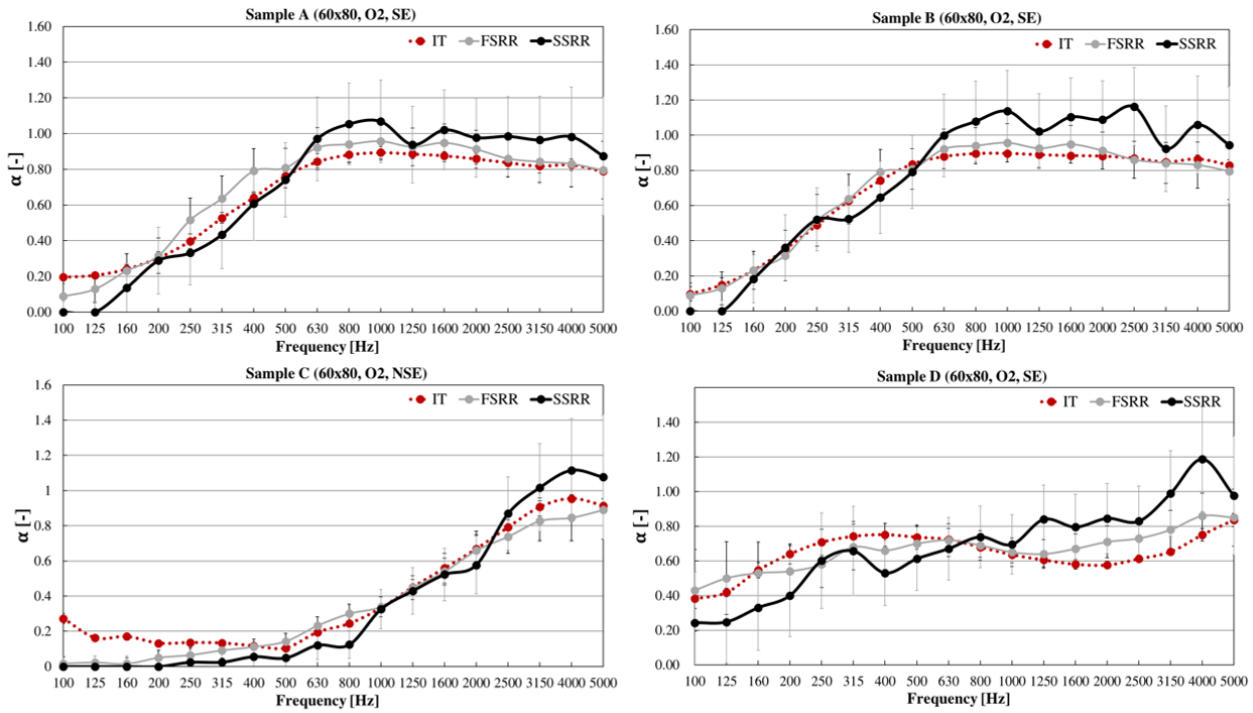
479

480   **Fig. 8.** Absorption coefficient of four materials in the conditions that minimized the normalized

481   error: samples with a size of 60×80 cm^2, orientation 2, with sealed edges (Sample A, B, and D) and

482   with unsealed edges (Sample C). Also, the FSRR data report measurements with sealed edges and

483   no sealed edges, respectively. IT data are given after correction for diffuse incidence.

484
485

486   *4.3* Single number acoustic indices α_w, NRC, and SAA

487   Based on the above results, sound absorption indices α_w, NRC, and SAA are derived from the IT,

488   FSRR and SSRR measurements. These single indices are useful for an immediate and practical

489   comparison of the performance of different materials. The higher the α_w, SAA or the NRC values,

490   the better is the material capability in sound absorption. Their values normally range from 0 to 1,

491   with 1 meaning 100% sound absorption for 1 m^2 of material. These three indices have been

492   compared in former studies in order to estimate the differences and any possible drawback that

493   could lead to flaws in the performance comparison [47].

494   The weighted sound absorption coefficient α_w is derived from practical sound absorption

495   coefficients, α_p. They are frequency-dependent values of the sound absorption coefficient, based on

496   measurements on one-third octave bands (according to EN ISO 354 [2]) and calculated in octave

497   bands in accordance with EN ISO 11654 [48]. An averaged α_p is calculated for the three one-third

498   octave sound absorption coefficients within the octave. Weighted sound absorption coefficient α_w

499   can be obtained with the reference curve (α_{250}=0.8; α_{500}=1; α_{1000}=1; α_{2000}=1; α_{4000}=0.9). The curve is

500   shifted in steps of 0.05 towards the α_p values until the sum of unfavourable deviations (this occurs

501   when the measured value is lower than the value of the curve) is less or equal to 0.10. Finally, the

502   weighted sound absorption coefficient is the value of the adjusted reference curve at 500 Hz.

503   The single number rating obtained from ASTM C423 [3] is the Sound Absorption Average (SAA).

504   This is the average of the absorption coefficients for the twelve one-third octave bands from 200 Hz

505   to 2500 Hz. The SAA supersedes the Noise Reduction Coefficient (NRC), which is the arithmetic

506   average of the absorption coefficients determined at the octave bands of 250 Hz, 500 Hz, 1000 Hz

507   and 2000 Hz, rounded to the nearest multiple of 0.05. The SAA value is rounded off the nearest

508   0.01 increment. The ASTM standard does not introduce any shape indicators as the ISO method

509   described above.

510   The expanded uncertainty, at a confidence level of 95% (k=2), of the measured data under

511   reproducibility conditions for α_w has been evaluated according to Wittstock (2018) [43] and is equal

512   to 0.07, i.e. twice the reproducibility standard deviation; the same value has been considered also

513   for SAA and NRC, since no information is given on this regard in literature. As can be noticed in

514   table 2, there are a few differences among the single indices within each material data. The

515   differences SSRR and FSRR related to α_w are within a 0.10 for samples A and B, and 0.05 for

516   samples C and D; differences related to NRC and SAA are within 0.05 for all the samples. Table 2

517   shows also the normalized error which has been evaluated for IT and SSRR measurements with

518   respect to the FSRR data and SSRR with respect to the IT single values. The results can be

519   considered compatible in most of the cases ($E_n < 1$). However, it can be noticed that the differences

520   between SSRR and FSRR are comparable to those between IT and FSRR.

521

522   Table 2: Comparison of results of single acoustic indices (NRC, SAA and α_w) for the four samples

523   (A, B, C, D) and three different test methods (IT, FSRR, and SSRR). Normalized error of the IT and

524   SSRR measurements with respect to the FSRR data and SSRR measurements with respect to IT

525   data. $E_n > 1$ are indicated in bold.

Sample	A			B			C			D		
Test Method	α_w	SAA	NRC	α_w	SAA	NRC	α_w	SAA	NRC	α_w	SAA	NRC
IT	0.70	0.73	0.75	0.75	0.77	0.75	0.20	0.32	0.30	0.65	0.67	0.65
FSRR	0.75	0.79	0.75	0.85	0.84	0.75	0.20	0.31	0.30	0.70	0.66	0.70
SSRR	0.65	0.78	0.80	0.75	0.87	0.85	0.15	0.26	0.25	0.70	0.68	0.70
$E_{n\,(IT\text{-}FSRR)}$	0.51	0.61	0.00	**1.01**	0.71	0.00	0.00	0.10	0.00	0.51	0.10	0.51
$E_{n\,(SSRR\text{-}FSRR)}$	**1.01**	0.10	0.51	**1.01**	0.30	**1.01**	0.51	0.51	0.51	0.00	0.20	0.00
$E_{n\,(SSRR\text{-}IT)}$	0.51	0.51	0.51	0.00	**1.01**	**1.01**	0.51	0.61	0.51	0.51	0.10	0.51

526
527
528   *4.4 Comparison among the three methods*

529   Finally, a summary of the advantages and disadvantages of the three methods are listed in Table 3.

530   It can be noticed that the SSRR presents a series of practical advantages that could allow for faster

531   measurements applying less resources, i.e. allows for an explorative phase in the early stages of the

532   design process as well as reduces the amount of material used for the production of the samples

533   leading to more sustainable ways of performing acoustic measurements. Moreover, these practical

534   features and faster feedback could ease the dissemination and increase awareness related to the

535   acoustic performance among designers and architects.

536   **5 Conclusions**

537   This work explored the range of application and reliability of the random-incidence absorption

538   coefficient measured within a small-scale reverberation room. Four different materials have been

539   measured with three different methods in the impedance tube (IT), full-scale (FSRR) and small-

scale (SSRR) reverberation room. It was shown that the SSRR presents several advantages compared to the other methods, which have a practical relevance in the explorative design process of sound absorptive building materials. After the research and development phase, the final material can be sent to an independent acoustical laboratory for qualified ISO 354:2003 measurements.

Table 3: Synthetic comparison among IT, FSRR and SSRR methods.

Method	Sound incidence	Frequency range [Hz]	Sample area (m^2)	Advantages	Disadvantages
IT	Normal	100-5000 (depending on the tube diameter)	< 0.1	• reduced sample size • affordable measurement costs • limited wasted material • measurement time duration (< 30 min)	• limited frequency range • normal sound incidence • 3D absorbing systems
FSRR	Random	100-5000	10-12	• sound incidence • limited edge effect • broad frequency range • 3D absorbing systems	• large sample size • huge measurement costs • high quantity of material to be dismantled • measurement time duration (> 60 min)
SSRR	Random	400-5000 (for porous materials) 1000-5000 (for thin rigid materials)	0.2-1.5	• sound incidence • reduced sample size • affordable measurement costs • limited wasted material • measurement time duration (<30 min) • 3D absorbing systems	• limited lower frequency range • edge effect • limited sample height

The SSRR-based results have been compared against FSRR measurement, used as a reference, and IT measurements. The analyses showed that normalized errors smaller than 1 – i.e. compatible results – can be generally achieved, provided that some recommendations in measurement setup are needed. First, to have reliable data a sample size close to 60×80 cm^2 is recommended; the size

should be placed with an oblique orientation on the room floor. Second, the sound absorption coefficients data showed that the edge effect is more evident for thicker panels (>50cm) and smaller samples ($60x40cm^2$). For samples sizes of $60x80cm^2$ the edge effect has been shown to be reduced also for thicker samples. This aspect should be investigated in a more systematic way including panels with thicknesses above those considered here in order to find a threshold of validity due to this parameter. Third, a sound absorption overestimation can take place depending on the sample thickness. Fourth, due to the limited diffusivity of the sound field, the SSRR method can be profitably adopted when the frequencies of interest lie above 400 Hz for porous materials and above 1000 Hz for thin low absorptive rigid materials. Nevertheless, as previously stated, since larger uncertainties in SSRRs and in FSRRs might occur especially for higher absorptive materials with ISO 354 method [43], compatibility ranges could be wider. Future research will be aimed at investigating this aspect.

Within these use-cases, the discussed results show that that the small reverberation room is a reliable measurement tool in the frequency range 400-5000 Hz (for porous materials) and 1000-5000 Hz (for thin rigid materials), and therefore, can be considered as a valid alternative to the measurements in the full-scale or in the impedance tube. These might require a more systematic study that would consider also other variables (e.g. room volume variations) in order to define the proper range of application.

Finally, this work has pointed out the advantages related to the possibility to test small-size samples, thus potentially leading to limited wasted material and transportation costs for the tested samples. Moreover, the sample arrangement in the SSRR set-up requires a shorter time, enabling in turn to dedicate an increased time to test different alternatives. Moreover, this could ease the dissemination and increase awareness related to the acoustic performance among designers and architects while pursuing more sustainable ways to perform acoustic measurements.

583

584 **References**
585

586 [1] ISO 10534-2:1998, Acoustics - Determination of sound absorption coefficient and impedance in

587   impedance tubes - Part 2: Transfer-function method. International Organization for

588   Standardization, Geneva, Switzerland.

589 [2] ISO 354:2003, Acoustics - measurement of sound absorption in a reverberation room.

590   International Organization for Standardization, Geneva, Switzerland.

591 [3] ASTM C423-17:2017, Standard Test Method for Sound Absorption and Sound Absorption

592   Coefficients by the Reverberation Room Method, ASTM International, West Conshohocken,

593   PA.

594 [4] A. Alonso, F. Martellotta, Room acoustic modelling of textile materials hung freely in space:

595   from the reverberation chamber to ancient churches, Journal of Building Performance Simulation

596   9 (2016), 469-486. http://dx.doi.org/10.1080/19401493.2015.1087594

597 [5] J. R.Veen, J. Pan, P. Saha, Development of a Small Size Reverberation Room Standardized Test

598   Procedure for Random Incidence Sound Absorption Testing, Proc. SAE conference 2005,

599   Traverse City, USA, 2005.

600 [6] SAE j2883:2015 - Laboratory Measurement of Random Incidence Sound Absorption Tests Using

601   a Small Reverberation Room. SAE International.

602 [7] P. Jackson, Design and Construction of a Small Reverberation Chamber, Proc. SAE conference

603   2005, Traverse City, USA, 2005.

604 [8] G. Baldinelli, F. Bianchi, S. Endelis, A. Jakovics, G. L. Morini, S. Falcioni, S. Fantucci, V. Serra,

605   M. A. Navacerrada, C. Díaz, A. Libbra, A. Muscio, F. Asdrubali, Thermal conductivity

606   measurement of insulating innovative building materials by hot plate and heat flow meter

607   devices: a round Robin test. Int. J. Therm. Sci. 139 (2019), 25-35.

608   https://doi.org/10.1016/j.ijthermalsci.2019.01.037

609 [9] R. Del Rey, J. Alba, L. Bertó, A. Gregoriù, Small-sized reverberation chamber for the

610   measurement of sound absorption, Materiales de Construcción 67 (2017), 139.

611   http://dx.doi.org/10.3989/mc.2017.07316

612 [10] L. Pacheco Bastos, G. Da Silva Vieira de Melo, N. Sure Soeiro, Panels Manufactured from

613   Vegetable Fibers: An Alternative Approach for Controlling Noises in Indoor Environments,

614   Advances in acoustic and vibration 2012, (paper 698737).

615   http://dx.doi.org/10.1155/2012/698737

616 [11] M. Kierzkowski, H. Law, J. Cotterill, Benefits of Reduced-size Reverberation Room Testing.

617   Proc. Acoustics 2017, Perth, Australia, 2017.

618 [12] A. Rasa, Development of a small-scale reverberation room, Proc. Acoustics 2016, Brisbane,

619   Australia, 2016.

620 [13] A. Chappuis, Small size devices for accurate acoustical measurements of materials and parts

621   used in automobiles, Proc. SAE conference 1993; Traverse City, USA, 1993.

622 [14] A. De Bruijn, On the scattering of a plane wave by porous sound-absorbing strip, Proc.

623   Euronoise 2008, Paris, France, 2008.

624 [15] A. Duval, J.-F. Rondwau, L. Dejaeger, F. Sgard, N. Atalla, Diffuse field absorption coefficient

625   simulation of porous materials in small reverberant chambers: finite size and diffusivity issues,

626   Proc. Congres Francais d'Acoustique 2010, Lyon, France, 2010.

627 [16] A. Cops, J. Vanhaecht, K. Leppens, Sound Absorption in a Reverberation Room: Causes of

628   Discrepancies on Measurement Results, Appl. Acoust. 46 (1995), 215-232.

629   https://doi.org/10.1016/0003-682X(95)00029-9

630 [17] M. Nolan, M. Vercammen, C. H. Jeong, Effects of different diffusers types on the diffusivity in

631   reverberation chambers, Proc. Euronoise 2018, Crete, Greece, 2018.

632 [18] D. T. Bradley, M. Müller-Trapet, J. Adelgren, M. Vorländer, Effect of boundary diffusers in a

633 reverberation chamber: Standardized diffuse field quantifiers. J. Acoust. Soc. Am. 135 (2014),

634 1898-1906. https://doi.org/10.1121/1.4866291

635 [19] T.J. Cox, P. D'Antonio, Acoustic Absorbers and Diffusers: Theory, Design and Application,

636 Spon Press, London, United Kingdom, 2004.

637 [20] C. Scrosati, F. Scamoni, M. Depalma, N. Granzotto, On the diffusion of the sound field in a

638 reverberation room, Proc. 26th International Congress on Sound and Vibration, ICSV, Montréal,

639 Canada, 2019.

640 [21] M. Vercammen, Improving the accuracy of sound absorption measurements according to ISO

641 354, Proc. ISRA 2010, Melbourne, Australia 2010.

642 [22] W. A. Davern, P. Dubout, First report on Australasian comparison measurements of sound

643 absorption coefficients, Proc. CSIRIO 1980, Melbourne, 1980.

644 [23] N.B. Roozen, E.A. Piana, E. Deckers, C. Scrosati, On the numerical modelling of reverberant

645 rooms, including a comparison with experiments, Proc. ICSV 2019, Montréal, Canada, 2019.

646 [24] M. Nolan, M. Vercammen, C. H. Jeong, J. Brunskog, The Use of a Reference Absorber for

647 Absorption Measurements in a Reverberation Chamber, Proc. Forum Acusticum 2014, Krakow,

648 Poland, 2014.

649 [25] C. Scrosati, D. Annesi, L. Barbaresi, R. Baruffa, F. D'Angelo, G. De Napoli, M. Depalma, A. Di

650 Bella, S. Di Filippo, D. D'Orazio, M. Garai, N. Granzotto, V. Lori, F. Martellotta, A. Moschetto,

651 F. Pompoli, A. Prato, P. Nataletti, F. Scamoni, A. Schiavi, F. Serpilli, Design Principles of the

652 Italian Round Robin Test on Reverberation Rooms, Proc. of ICA 2019, Aachen, Germany, 2019.

653 [26] A. Prato, F. Casassa, A. Schiavi, Reverberation time measurements in non-diffuse acoustic field

654 by the modal reverberation time, Appl. Acoust. 110 (2016), 160-169.

655 https://doi.org/10.1016/j.apacoust.2016.03.041

656 [27] S. De Cesaris, D. D'Orazio, F. Morandi, M. Garai, Extraction of the envelope from impulse

657   responses using pre-processed energy detection for early decay estimations, J. Acoust. Soc. Am.

658   138 (2015), 2513-2523. https://doi.org/10.1121/1.4931904

659 [28] J. R. Veen, P. Saha, Feasibility of a standardized test procedure for random incidence sound

660   absorption tests using a small size reverberation room, Proc. SAE conference 2003, Traverse

661   City, USA, 2003.

662 [29] T. W. Bartel, Effect of absorber geometry on apparent absorption coefficients as measured in a

663   reverberation   chamber,   J.   Acoust.   Soc.   Am.   69   (1981),   1065-1074.

664   https://doi.org/10.1121/1.385685

665 [30] F. Pompoli, P. Bonfiglio, K. V. Horoshenkov, A. Khan, L. Jaouen, F. Bécot, F. Sgard, F.

666   Asdrubali, F. D'Alessandro, J. Hübelt, N. Atalla, C. K. Amédin, W. Lauriks, L. Boeckx, How

667   reproducible is the acoustical characterization of porous media?, J. Acoust. Soc. Am. 141 (2017),

668   945-955. https://doi.org/10.1121/1.4976087

669 [31] D. Pilon, R. Panneton, F. Sgard, Behavioural criterion quantifying the effects of circumferential

670   air gaps on porous materials in the standing wave tube, J. Acoust. Soc. Am. 116 (2004), 344-356.

671   https://doi.org/10.1121/1.1756611

672 [32] R. Spagnolo, G. Benedetto, Reverberation time in enclosures: The surface reflection law and the

673   dependence of the absorption coefficient on the angle of incidence, J. Acoust. Soc. Am. 77

674   (1985), 1447-1451. https://doi.org/10.1121/1.392039

675 [33] P. Bonfiglio, F. Pompoli, R. Lionti, A reduced-order integral formulation to account for the

676   finite size effect of isotropic square panels using the transfer matrix method, J. Acoust. Soc. Am.

677   139 (2016), 1773-1783.

678 [34] C-H. Jeong, Non-uniform sound intensity distributions when measuring absorption coefficients

679   in reverberation chambers using a phased beam tracing. J. Acoust. Soc. Am. 127 (2010), 3560–

680   3568.

681 [35] ISO 9613:1993, Acoustics – attenuation of sound during propagation outdoors – Part 1:

682   calculation of the absorption of sound by the atmosphere. International Organization for

683   Standardization, Geneva, Switzerland.

684 [36] ISO 17497-1:2004, Acoustics – sound-scattering properties of surfaces – Part 1: measurement of

685   the random-incidence scattering coefficient in a reverberation room. International Organization

686   for Standardization, Geneva, Switzerland.

687 [37] L. Shtrepi, A. Astolfi, G. D'Antonio, G. Vannelli, G. Barbato, S. Mauro, A. Prato, Accuracy of

688   the random-incidence scattering coefficient measurement. Appl. Acoust. 106 (2016), 23-35.

689   https://doi.org/10.1016/j.apacoust.2015.12.021

690 [38] C. -H. Jeong, Diffuse Sound Field: Challenges and Misconceptions. Proc. INTER-NOISE 2016,

691   Hamburg, Germany.

692 [39] A. Gerbotto, Caratterizzazione di una camera riverberante in scala - Acoustic characterization of

693   a scaled reverberation room, Master Thesis, Politecnico di Torino, 2016.

694 [40] ITA-Toolbox for MATLAB® Developed at the Institute of Technical Acoustics at RWTH

695   Aachen University.

696 [41] ISO/IEC 17043:2010, Conformity assessment - General requirements for proficiency testing.

697   International Organization for Standardization, Geneva, Switzerland.

698 [42] JCGM 100 2008 Evaluation of Measurement Data — Guide to the Expression of Uncertainty in

699   Measurement (*GUM)*, Joint Committee for Guides in Metrology, Sèvres, France.

700 [43] V. Wittstock, Determination of Measurement Uncertainties in Building Acoustics by

701   Interlaboratory Tests. Part 2: Sound Absorption Measured in Reverberation Rooms, Acta Acust.

702   United with Acust. 104 (2018), 999 – 1008. https://doi.org/10.3813/AAA.919266

703 [44] D. George, P. Mallery, SPSS for Windows Step by Step: A Simple Guide and Reference 17.0

704   Update. 10th Edition, Pearson, Boston, 2010.

705   [45] A. Schiavi and A. Prato, Valuation of sound absoprtion: an experimental comparative study

706   among reverberation room, impedance tube and airflow resistivity-based models, Proc. ICSV

707   2019, Montréal, Canada, 2019.

708   [46] Jain, S., Joshi, M., Bankar, H., Kamble, P., Yadav P., Karanth N. Measurement and Prediction

709   of Sound Absorption of Sound Package Materials in Large and Small Reverberation Chambers,

710   Proc SAE conference 2017, Traverse City, USA, 2017.

711   [47] J. Białek, E. Nowicka, Comparison of sound absorption ratings calculated according to ISO and

712   ASTM standards, Proc. OSA 2016, Warsaw, Poland, 2016.

713   [48] ISO 11654:1997, Acoustics - Sound absorbers for use in buildings - Rating of sound absorption.

714   International Organization for Standardization, Geneva, Switzerland.

Appendix A
Sound absorption coefficient (α_s) and related uncertainty (U) for material A measured in SSRR, IT and FSRR. Given the background noise criterion (section 2.4), the SSRR data are valid for 250-5000 Hz. IT_n shows the data for normal-incidence sound absorption coefficients.

SSRR			Frequency [Hz]																	
Size [cm²]	Orientation		100	125	160	200	250	315	400	500	630	800	1000	1250	1600	2000	2500	3150	4000	5000
60x40	O1	α_s	0.11	0.24	0.00	0.42	0.61	0.53	0.52	0.64	0.68	1.10	1.29	1.10	1.10	1.05	1.13	1.23	1.14	1.04
		U	0.17	0.23	0.06	0.24	0.28	0.22	0.18	0.19	0.18	0.24	0.27	0.24	0.23	0.23	0.24	0.28	0.30	0.35
	O2	α_s	0.10	0.20	0.00	0.40	0.60	0.48	0.53	0.60	0.68	1.03	1.15	1.20	1.20	0.96	1.21	1.10	1.17	0.94
		U	0.15	0.20	0.06	0.24	0.28	0.21	0.19	0.18	0.18	0.23	0.24	0.26	0.25	0.22	0.25	0.26	0.30	0.34
	O3	α_s	0.09	0.17	0.00	0.36	0.58	0.49	0.58	0.56	0.63	1.02	1.05	1.22	1.27	0.90	1.22	1.18	1.15	1.02
		U	0.15	0.18	0.06	0.22	0.27	0.21	0.20	0.17	0.17	0.22	0.23	0.26	0.26	0.21	0.25	0.27	0.30	0.35
60x60	O1	α_s	0.00	0.00	0.01	0.32	0.46	0.51	0.56	0.59	0.70	1.17	0.98	1.04	1.04	0.83	1.00	0.95	0.94	0.85
		U	0.06	0.06	0.06	0.20	0.23	0.21	0.19	0.18	0.19	0.25	0.22	0.23	0.23	0.20	0.22	0.24	0.27	0.33
	O2	α_s	0.00	0.00	0.04	0.33	0.47	0.47	0.58	0.63	0.80	1.06	1.00	1.06	0.96	0.86	1.00	0.92	1.07	0.91
		U	0.06	0.06	0.08	0.21	0.23	0.20	0.20	0.19	0.20	0.23	0.22	0.23	0.21	0.20	0.22	0.24	0.29	0.33
60x80	O1	α_s	0.00	0.00	0.18	0.26	0.38	0.49	0.57	0.72	0.96	1.04	1.08	1.02	1.09	0.92	0.96	0.95	0.97	0.85
		U	0.06	0.06	0.16	0.18	0.20	0.21	0.20	0.20	0.23	0.23	0.23	0.23	0.23	0.21	0.22	0.24	0.28	0.33
	O2	α_s	0.00	0.00	0.14	0.29	0.33	0.43	0.61	0.74	0.97	1.05	1.07	0.94	1.02	0.98	0.98	0.96	0.98	0.87
		U	0.06	0.06	0.14	0.19	0.18	0.19	0.21	0.21	0.23	0.23	0.23	0.21	0.22	0.22	0.22	0.24	0.28	0.33
	O3	α_s	0.00	0.01	0.14	0.24	0.32	0.49	0.56	0.73	0.85	1.07	1.03	0.94	1.05	0.88	0.95	0.92	0.98	0.88
		U	0.06	0.07	0.14	0.16	0.18	0.21	0.19	0.21	0.21	0.23	0.23	0.21	0.23	0.21	0.22	0.24	0.28	0.33
IT		α	0.20	0.21	0.24	0.30	0.40	0.53	0.64	0.76	0.84	0.88	0.89	0.89	0.88	0.86	0.84	0.82	0.83	0.79
		U	0.01	0.02	0.03	0.04	0.04	0.03	0.03	0.04	0.05	0.04	0.03	0.03	0.02	0.03	0.04	0.04	0.03	0.02
IT_n		α_0	0.14	0.15	0.17	0.22	0.30	0.42	0.53	0.66	0.76	0.81	0.83	0.82	0.80	0.78	0.75	0.73	0.74	0.69
		U	0.01	0.02	0.03	0.04	0.04	0.03	0.03	0.04	0.05	0.04	0.03	0.03	0.02	0.03	0.04	0.04	0.03	0.02
FSRR		α_s	0.09	0.13	0.23	0.32	0.52	0.64	0.79	0.81	0.92	0.94	0.96	0.93	0.95	0.91	0.86	0.84	0.83	0.79
		U	0.07	0.08	0.09	0.10	0.12	0.13	0.12	0.11	0.11	0.11	0.11	0.11	0.11	0.11	0.10	0.11	0.13	0.16

Appendix B
Sound absorption coefficient (α_s) and related uncertainty (U) for material B measured in SSRR, IT and FSRR. Given the background noise criterion (section 2.4), the SSRR data are valid for 250-5000 Hz. IT_n shows the data for normal-incidence sound absorption coefficients.

SSRR			Frequency [Hz]																
Size [cm^2]	Orientation		100	125	160	200	250	315	400	500	630	800	1000	1250	1600	2000	2500	3150	4000	5000
60x40	O1	α_s	0.11	0.24	0.00	0.42	0.61	0.53	0.52	0.64	0.68	1.10	1.29	1.10	1.10	1.05	1.13	1.23	1.14	1.04
		U	0.17	0.23	0.06	0.24	0.28	0.22	0.18	0.19	0.18	0.24	0.27	0.24	0.23	0.23	0.24	0.28	0.30	0.35
	O2	α_s	0.10	0.20	0.00	0.40	0.60	0.48	0.53	0.60	0.68	1.03	1.15	1.20	1.20	0.96	1.21	1.10	1.17	0.94
		U	0.15	0.20	0.06	0.24	0.28	0.21	0.19	0.18	0.18	0.23	0.24	0.26	0.25	0.22	0.25	0.26	0.30	0.34
	O3	α_s	0.09	0.17	0.00	0.36	0.58	0.49	0.58	0.56	0.63	1.02	1.05	1.22	1.27	0.90	1.22	1.18	1.15	1.02
		U	0.15	0.18	0.06	0.22	0.27	0.21	0.20	0.17	0.17	0.22	0.23	0.26	0.26	0.21	0.25	0.27	0.30	0.35
60x60	O1	α_s	0.00	0.00	0.01	0.32	0.46	0.51	0.56	0.59	0.70	1.17	0.98	1.04	1.04	0.83	1.00	0.95	0.94	0.85
		U	0.06	0.06	0.06	0.20	0.23	0.21	0.19	0.18	0.19	0.25	0.22	0.23	0.23	0.20	0.22	0.24	0.27	0.33
	O2	α_s	0.00	-0.09	0.04	0.33	0.47	0.47	0.58	0.63	0.80	1.06	1.00	1.06	0.96	0.86	1.00	0.92	1.07	0.91
		U	0.06	-0.01	0.08	0.21	0.23	0.20	0.20	0.19	0.20	0.23	0.22	0.23	0.21	0.20	0.22	0.24	0.29	0.33
60x80	O1	α_s	0.00	0.00	0.18	0.26	0.38	0.49	0.57	0.72	0.96	1.04	1.08	1.02	1.09	0.92	0.96	0.95	0.97	0.85
		U	0.06	0.06	0.16	0.18	0.20	0.21	0.20	0.20	0.23	0.23	0.23	0.23	0.23	0.21	0.22	0.24	0.28	0.33
	O2	α_s	0.00	0.00	0.14	0.29	0.33	0.43	0.61	0.74	0.97	1.05	1.07	0.94	1.02	0.98	0.98	0.96	0.98	0.87
		U	0.06	0.06	0.14	0.19	0.18	0.19	0.21	0.21	0.23	0.23	0.23	0.21	0.22	0.22	0.22	0.24	0.28	0.33
	O3	α_s	0.00	0.01	0.14	0.24	0.32	0.49	0.56	0.73	0.85	1.07	1.03	0.94	1.05	0.88	0.95	0.92	0.98	0.88
		U	0.06	0.07	0.14	0.16	0.18	0.21	0.19	0.21	0.21	0.23	0.23	0.21	0.23	0.21	0.22	0.24	0.28	0.33
IT		α	0.10	0.15	0.23	0.35	0.49	0.63	0.74	0.84	0.88	0.90	0.90	0.89	0.88	0.88	0.87	0.85	0.86	0.83
		U	0.04	0.04	0.02	0.00	0.01	0.01	0.01	0.01	0.01	0.01	0.01	0.01	0.01	0.01	0.01	0.01	0.02	0.03
IT_n		α_0	0.07	0.10	0.17	0.26	0.38	0.52	0.64	0.75	0.81	0.83	0.83	0.82	0.81	0.81	0.79	0.77	0.79	0.74
		U	0.04	0.04	0.02	0.00	0.01	0.01	0.01	0.01	0.01	0.01	0.01	0.01	0.01	0.01	0.01	0.01	0.02	0.03
FSRR		α_s	0.09	0.18	0.28	0.52	0.65	0.75	0.82	0.86	0.91	0.90	0.99	0.96	0.95	0.90	0.90	0.87	0.85	0.80
		U	0.07	0.09	0.11	0.14	0.15	0.14	0.13	0.12	0.11	0.10	0.11	0.11	0.11	0.10	0.11	0.12	0.13	0.16

Appendix C
Sound absorption coefficient (α_s) and related uncertainty (U) for material C measured in SSRR, IT and FSRR. Given the background noise criterion (section 2.4), the SSRR data are valid for 250-5000 Hz. IT_n shows the data for normal-incidence sound absorption coefficients.

SSRR			Frequency [Hz]																	
Size [cm^2]	Orientation		100	125	160	200	250	315	400	500	630	800	1000	1250	1600	2000	2500	3150	4000	5000
60x40	O1	α_s	0.00	0.00	0.00	0.01	0.03	0.02	0.02	0.07	0.10	0.12	0.32	0.38	1.12	1.12	1.12	1.07	1.21	0.98
		U	0.06	0.06	0.06	0.07	0.07	0.07	0.07	0.07	0.08	0.08	0.11	0.12	1.07	1.07	1.07	0.26	0.31	0.34
	O2	α_s	0.00	0.00	0.00	0.08	0.06	0.03	0.02	0.06	0.10	0.14	0.28	0.43	1.21	1.21	1.21	1.02	1.22	0.97
		U	0.06	0.06	0.06	0.09	0.08	0.07	0.06	0.07	0.08	0.08	0.11	0.13	1.18	1.18	1.18	0.25	0.31	0.34
	O3	α_s	0.00	0.00	0.00	0.09	0.07	0.03	0.04	0.08	0.11	0.09	0.30	0.51	1.32	1.32	1.32	1.03	1.15	0.97
		U	0.06	0.06	0.06	0.10	0.09	0.07	0.07	0.08	0.08	0.07	0.11	0.14	1.28	1.28	1.28	0.25	0.30	0.34
60x60	O1	α_s	0.02	0.05	0.05	0.03	0.10	0.04	0.03	0.08	0.11	0.14	0.34	0.46	0.50	0.54	0.82	0.93	1.02	1.02
		U	0.08	0.10	0.09	0.07	0.10	0.07	0.07	0.08	0.08	0.08	0.11	0.14	0.15	0.16	0.20	0.24	0.28	0.35
	O2	α_s	0.04	0.04	0.08	0.01	0.09	0.04	0.03	0.07	0.12	0.14	0.37	0.36	0.44	0.55	0.79	0.96	1.14	1.03
		U	0.10	0.09	0.10	0.06	0.09	0.07	0.07	0.07	0.08	0.08	0.12	0.12	0.14	0.16	0.20	0.24	0.30	0.35
60x80	O1	α_s	0.00	0.00	0.05	0.00	0.02	0.02	0.03	0.06	0.12	0.15	0.30	0.40	0.50	0.57	0.90	1.01	1.12	1.00
		U	0.06	0.06	0.09	0.06	0.07	0.06	0.07	0.07	0.08	0.08	0.11	0.13	0.15	0.16	0.21	0.25	0.29	0.34
	O2	α_s	0.00	0.00	0.00	0.00	0.02	0.03	0.06	0.05	0.12	0.12	0.33	0.43	0.52	0.58	0.87	1.02	1.12	1.08
		U	0.06	0.06	0.06	0.06	0.07	0.07	0.07	0.07	0.08	0.08	0.11	0.13	0.15	0.16	0.21	0.25	0.29	0.35
	O3	α_s	0.00	0.00	0.04	0.00	0.04	0.03	0.05	0.05	0.13	0.15	0.32	0.43	0.44	0.59	0.85	0.90	1.00	1.00
		U	0.06	0.06	0.08	0.06	0.08	0.07	0.07	0.07	0.08	0.08	0.11	0.13	0.14	0.17	0.21	0.24	0.28	0.34
IT		α	0.27	0.16	0.17	0.13	0.14	0.13	0.12	0.10	0.19	0.24	0.33	0.45	0.56	0.67	0.79	0.91	0.95	0.91
		U	0.03	0.02	0.02	0.01	0.01	0.00	0.00	0.00	0.00	0.01	0.02	0.04	0.08	0.10	0.07	0.05	0.01	0.04
IT_n		α_0	0.20	0.11	0.12	0.09	0.09	0.09	0.08	0.07	0.14	0.18	0.25	0.35	0.45	0.56	0.70	0.85	0.92	0.86
		U	0.03	0.02	0.02	0.01	0.01	0.00	0.00	0.00	0.00	0.01	0.02	0.04	0.08	0.10	0.07	0.05	0.01	0.04
FSRR		α_s	0.02	0.02	0.02	0.05	0.06	0.09	0.11	0.14	0.23	0.30	0.34	0.45	0.54	0.66	0.74	0.83	0.85	0.89
		U	0.04	0.04	0.03	0.04	0.04	0.04	0.04	0.04	0.05	0.05	0.06	0.07	0.08	0.09	0.10	0.11	0.13	0.17

Appendix D
Sound absorption coefficient (α_s) and related uncertainty (U) for material D measured in SSRR, IT and FSRR. Given the background noise criterion (section 2.4), the SSRR data are valid for 250-5000 Hz. IT_n shows the data for normal-incidence sound absorption coefficients.

SSRR			Frequency [Hz]																	
Size [cm^2]	Orientation		100	125	160	200	250	315	400	500	630	800	1000	1250	1600	2000	2500	3150	4000	5000
60x40	O1	α_s	0.07	0.28	0.39	0.65	0.78	0.98	1.07	0.74	1.00	1.21	1.36	0.90	0.85	0.95	1.00	1.21	1.20	1.01
		U	0.12	0.26	0.28	0.35	0.34	0.35	0.32	0.21	0.24	0.25	0.28	0.21	0.20	0.22	0.22	0.27	0.30	0.35
	O2	α_s	0.03	0.26	0.38	0.72	0.79	0.93	0.85	0.70	0.94	1.11	1.29	0.88	1.03	0.90	1.05	1.13	1.25	1.10
		U	0.09	0.25	0.27	0.38	0.34	0.34	0.26	0.20	0.23	0.24	0.27	0.20	0.22	0.21	0.23	0.26	0.31	0.35
	O3	α_s	0.00	0.26	0.40	0.70	0.88	0.92	0.90	0.72	0.94	1.19	1.13	0.99	1.02	0.87	0.99	1.04	1.28	0.96
		U	0.06	0.25	0.29	0.37	0.38	0.34	0.28	0.20	0.23	0.25	0.24	0.22	0.22	0.21	0.22	0.25	0.31	0.34
60x60	O1	α_s	0.09	0.37	0.35	0.53	0.68	0.67	0.58	0.67	0.75	0.93	0.91	0.84	0.78	0.98	0.96	0.98	1.26	1.07
		U	0.14	0.33	0.26	0.29	0.30	0.26	0.20	0.19	0.20	0.21	0.21	0.20	0.19	0.22	0.22	0.25	0.31	0.35
	O2	α_s	0.20	0.41	0.37	0.54	0.59	0.67	0.64	0.61	0.76	1.04	0.84	0.87	1.02	0.87	0.97	1.05	1.25	1.09
		U	0.25	0.35	0.27	0.30	0.27	0.26	0.21	0.18	0.20	0.23	0.19	0.20	0.22	0.21	0.22	0.25	0.31	0.35
60x80	O1	α_s	0.15	0.24	0.34	0.33	0.47	0.66	0.53	0.69	0.70	0.69	0.73	0.71	0.72	0.76	0.80	1.05	1.12	0.99
		U	0.21	0.23	0.25	0.21	0.23	0.26	0.19	0.20	0.19	0.17	0.18	0.18	0.18	0.19	0.20	0.25	0.29	0.34
	O2	α_s	0.24	0.25	0.33	0.40	0.60	0.66	0.53	0.61	0.67	0.74	0.69	0.84	0.80	0.85	0.83	0.99	1.19	0.98
		U	0.29	0.24	0.24	0.24	0.28	0.26	0.19	0.18	0.18	0.18	0.17	0.20	0.19	0.20	0.20	0.25	0.30	0.34
	O3	α_s	0.14	0.26	0.38	0.43	0.54	0.65	0.66	0.78	0.68	0.70	0.73	0.59	0.76	0.85	0.86	0.98	1.11	0.92
		U	0.19	0.25	0.27	0.25	0.25	0.26	0.22	0.22	0.18	0.17	0.18	0.16	0.18	0.20	0.21	0.25	0.29	0.34
IT		α	0.38	0.42	0.55	0.64	0.71	0.74	0.75	0.74	0.72	0.68	0.64	0.61	0.58	0.58	0.61	0.65	0.75	0.84
		U	0.06	0.02	0.04	0.06	0.08	0.08	0.07	0.07	0.06	0.06	0.05	0.04	0.03	0.02	0.02	0.01	0.04	0.04
IT_n		α_0	0.29	0.32	0.44	0.53	0.60	0.64	0.65	0.63	0.62	0.57	0.53	0.50	0.47	0.47	0.50	0.54	0.65	0.75
		U	0.06	0.02	0.04	0.06	0.08	0.08	0.07	0.07	0.06	0.06	0.05	0.04	0.03	0.02	0.02	0.01	0.04	0.04
FSRR		α_s	0.43	0.50	0.53	0.54	0.58	0.68	0.66	0.70	0.72	0.69	0.65	0.64	0.67	0.71	0.73	0.78	0.86	0.85
		U	0.24	0.21	0.18	0.15	0.13	0.13	0.11	0.10	0.09	0.09	0.08	0.08	0.09	0.09	0.10	0.11	0.13	0.16